Geochemical Perspectives Letters EAG

Subduction of sedimentary carbonate in the Mariana trench

S. Liu, X. Su, S. Wan, L. Zhang, S. Chen, W. Xu, H. Xu, D. Wang, D. Li, X. Peng

Supplementary Information

The Supplementary Information includes:

- Background and sampling
- Methods
- Tables S-1 to S-4
- Figures S-1 to S-5
- Supplementary Information References

Background and sampling

The Challenge Deep in the southwest of the Mariana Trench (MT), formed as the Pacific Plate subducts beneath the Philippine Plate, represents the deepest part of the Earth's ocean, with a maximum water depth of 10908 m. During the TS21 cruise of the R/V TanSuoYiHao in September-November 2021 at the MT, we conducted twenty-nine dives using the human operation vehicle (HOV) *Fendouzhe*. Initially aimed at investigating the geology, environment, and life of the MT, these dives unexpectedly revealed carbonate deposits during three of them, with water depths ranging from 6675 to 10812 m (Fig. 1 and Table S-1). These deposits became the primary focus of the present study.

A sediment core sample, measuring 21 cm in length, was collected with push corers at site FDZ050, while relatively consolidated surface sediment samples were obtained with the manipulator of the HOV at sites FDZ065 and JL147. Station locations are indicated in Figure 1 and Table S-1. Immediately after recovery, the collected samples were transferred to the ship's cold room (4 ℃) and sectioned for further analysis. Pore-water from nearby sites was collected using Rhizon samplers for subsequent geochemical analyses. Visual observations and video footage obtained during the dives were utilised to investigate the distribution of the carbonate deposits. The areas of these deposits were roughly estimated using the laser markers' scale (spaced 10 cm apart) on the capture images from the dive video (Table S-1). Expeditions and samplings were done with the permission of the Federated States of Micronesia.

Methods

Biogenic deposits analysis and age determination

Identification of calcareous nannofossils was carried out using a combination of an optical microscope and SEM. Samples were prepared as smear slides following Bown (1998), mounted with Norland optical adhesive, and examined with an Olympus BX53 light microscope at×1000 magnification. Each field of view was examined in both cross-polarised light and phase contrast for an accurate check of different taxa. The calcareous nannofossil taxonomic concepts primarily follow Bown (1998), and the calibrated ages of bio-events of Gradstein *et al.*, (2020) were used. Full taxonomic citations and bibliographic references for all taxa can be found on the Nannotax website (http://www.mikrotax.org/Nannotax3/). SEM analyses were performed with a Thermo Scientific Apreo C at the Institute of Deep-Sea Science and Engineering (IDSSE; Chinese Academy of Sciences), equipped with an energy-dispersive X-ray-detector for element analysis.

Age control was established by the biostratigraphic zonation scheme (Gradstein *et al.*, 2020) and strontium isotopes of bulk carbonate (McArthur *et al.*, 2001). Each weighted (~0.10 g) sediment was made into several radiolarian sample slides following the methods of Qiu *et al.* (2021). Identification of radiolarian species was carried out using a biological microscope, Nikon E200 at ×100 or ×200 magnification. Age control was established by Cenozoic radiolarian stratigraphy for low and middle latitudes with descriptions of biomarkers and stratigraphically useful species (Nigrini and Sanfilippo, 2001; Nigrini *et al.*, 2005). Identification of planktonic foraminifera was achieved using the optical microscope of ZEISS Stemi 508. Relevant age constraints of planktonic foraminifera were referred to the biostratigraphic zonation scheme (Gradstein *et al.*, 2020).

Geochemical analyses

Porosity is determined by drying the sediment. Wet sediment was weighed, freeze-dried and weighed again. The porosity (φ) was calculated from the difference of the two weights. Density is simply the weight of sediments, measured after evaporating interstitial water, divided by the initial volume of the sample.

The mineral compositions of bulk sediment samples were determined using a Bruker D8 Advance X-ray diffractometer (XRD) at IDSSE. The XRD was operated with a scanning speed of 2°/min between 5° and 80°. Mineral identification and analysis were conducted using the HighScore software from Malvern Panalytical.

The carbonate content of the bulk sediments was determined gravimetrically as loss on ignition (LOI) following the procedures outlined by Heiri *et al.* (2001). For the analysis of $\delta^{13}C$ and $\delta^{18}O$ values in calcareous sediments, a stable isotope mass spectrometer (Thermo Delta V Advantages) at the State Key Laboratory of Marine Geology, Tongji University, was employed. The analytical accuracy was better than ±0.1‰. For Sr isotopic ratios, measurements were performed using a Thermo Triton TIMS. The $^{87}Sr/^{86}Sr$ values were corrected for instrumental mass fractionation by $^{88}Sr/^{86}Sr = 8.375209$. The Sr isotope results are reported relative to SRM 987 of $^{87}Sr/^{86}Sr = 0.710248$. Rock standards BHVO-2 ($^{87}Sr/^{86}Sr = 0.703506 \pm 5$, 2SE), AGV-2 (0.703976 ± 7), JB-3 (0.703432 ± 7), and W-2A (0.706952 ± 7) were prepared and measured along with the unknowns to monitor the quality of Sr analyses.

Modeling and calculating

Saturation indexes calculation

Using the Excel CO2calc program (Robbins *et al.*, 2010), we calculated saturation indexes for calcite (Ωcalc) and aragonite (Ωarag) of ambient seawater from sampling sites and pore-water from nearby cores. The key parameters utilised for the model calculations and corresponding results can be found in Table S2.

Calculation of carbon content

Carbon mass in carbonate sediments, denoted as M_C, was calculated using the methods outlined by Rea and Ruff (1996) and Plank and Langmuir (1998): M_C=t(1-θ) ρw*12 %, where t is sediment thickness from the seismic (400 m), as reported by Clift, (2017). θ is the sediment porosity (82 %), and ρ is the sediment density (1.7 g/cm^3). The parameter 'w' represents the calcium carbonate, accounting for approximately 70 % of the total sediment weight. 12 % is the mass fraction of carbon in carbonate. The distribution area of carbonate sediments is estimated to be 1080 km^2 using Global Mapper software. The calculation of carbon content here is re relatively conservative as the thickness of the sediment used for calculation represents only a portion of the entire sediment column. Flux can be calculated by multiplying mass with the trench length (L) and the subduction rate (r). It's worth nothing that these values may represent an upper limit of sedimentary inorganic carbon subduction flux, due to the uneven distribution of carbonate sediments.

In detail, *Mc* = 400 m*(1-82 %) *1.7 g/cm^3 * 70% * 12 % = 1028.16 g/cm^2,

The total amount of carbon discovered in study: 1028.16 g/cm^2 * 1080km^2 = 1.11*10^{16} g

Flux = *Mc**L*r = 1028.16 g/cm^2 * 1400 km * 4.75 cm/ year = 68.4*10^4 Mt/Ma

We also calculated the flux of carbonate from ODP Site 800 and Site 801 using the same formula. The average carbonate content in sediments at Sites 800 and 801 is 2.5 % (data from site 800 and 801 Initial Report). To facilitate comparison with our values, sediment porosity and density are assumed to be consistent with ours.

Mc = 400 m*(1-82 %) *1.7 g/cm^3 * 2.5% * 12% = 36.72 g/cm^2

Flux = *Mc**L*r = 36.72 g/cm^2 * 1400 km * 4.75 cm/ year = 2.4*10^4 Mt/Ma

Supplementary Tables

Table S-1 Station characteristics and sampling details

Site	Device	Core length (cm)	Water Depth (m)	Longitude (°)	Latitude (°)	Areas (m^2)
FDZ050	HOV	21	10813	142.60	11.37	<1
FDZ065	HOV	surface	8247	141.82	11.14	>200
JL147	HOV	surface	6675	141.98	10.96	<1

Table S-2 Ambient seawater composition and saturation indexes of calcite and aragonite near the FDZ050 site were calculated using the CO_2calc program developed by *Robbins et al.* (2010).

Parameters	Value	Unit
Salinity	34.7	‰
Temperature	1.4	°C
Pressure	10813	dbars
PO_4^{3-}	2.5	µmol/L
Ca^{2+}	11.8	mmol/L
pH	7.9	
Alkanity	3.2	mmol/L
$\boldsymbol{\Omega_{calc}}$	0.66	
$\boldsymbol{\Omega_{arag}}$	0.48	

Table S-3 Isotope compositions (O, C, and Sr) of carbonate samples from the MT. nd: not determined.

Sample	(*n*)	$\delta^{13}C \pm SD$ (‰ VPDB)	$\delta^{18}O \pm SD$ (‰ VPDB)	$^{87}Sr/^{86}Sr$
FDZ050 (4cm)	3	1.81±0.04	0.53±0.08	0.708499±0.000006
FDZ050 (8cm)	3	1.76±0.04	0.64±0.03	0.708461±0.000006
FDZ050 (18cm)	3	1.85±0.04	0.55±0.11	0.708522±0.000005
FDZ065 (bulk)	3	1.43±0.05	-0.58±0.10	0.708383±0.000006
FDZ065 (pic foraminifer)	3	1.57±0.03	-0.85±0.06	nd

Table S-4 The genera and epochs of microfossils in the samples.

Site	Depth (cm)	Species	Grouped Taxa	Ages(Ma) First occurrence	Ages(Ma) Last occurrence
FDZ050	8	Calcareous nannofossils	*Discoaster signus*	17.95	13.53
	8		*Reticulo fenestra* spp	50.5	2.59
	21		*Coccolithus pelagicus*	65.4	0
	21		*Coronocyclus nitescens*	46.29	12.1
	21		*Sphenolithus moriformis*	61.61	3.92
	8,21		*Cyclicargolithus floridanus*	46.29	11.85
	8,21		*Discoaster deflandrei*	55.86	10.89
	8,21		***Discoaster exilis***	17.39	10.49
	8,21		***Sphenolithus heteromorphus***	17.71	13.53
	2	Radiolarian	***Buccinosphaera invaginata***	0.34	Extant
	8		*Calocycletta mizutamiensis*	Early mid-Miocene	
	12		*Trissocyclus stauroporus*	-	15.03
			Carpocanium rubyae	-	13.62
			Eucyrrtidium diaphanes	22.95	14.75
			Calocycletta virginis (*Riedel et Sanfilippo*)	21.12	12.72
	12,21		***Calocycletta costata(Riedel)***	17.6	13.44
FDZ065	0	Foraminifera	*Globoturborotalita euapertura*	Oligocene - early Miocene	
	0		*Dentoglobigerina globularis*		
FDZ050	8		*Paragloborotalia siakensis*	30.28	10.46

Supplementary Figures

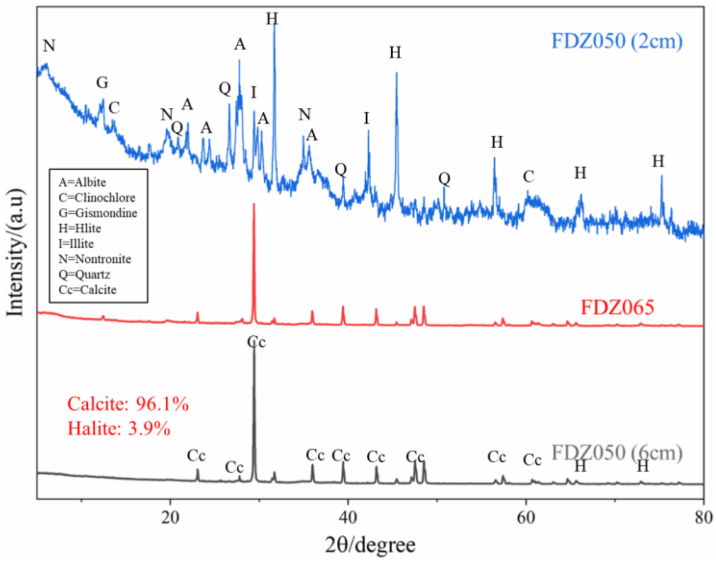

Figure S-1 XRD analysis of sediment samples in the study. The blue spectrum represents pelagic brown clay sediment from a 2 cm depth at site FDZ050. The red and gray spectra represent calcite from sites FDZ065 and FDZ050 (6 cm depth), respectively.

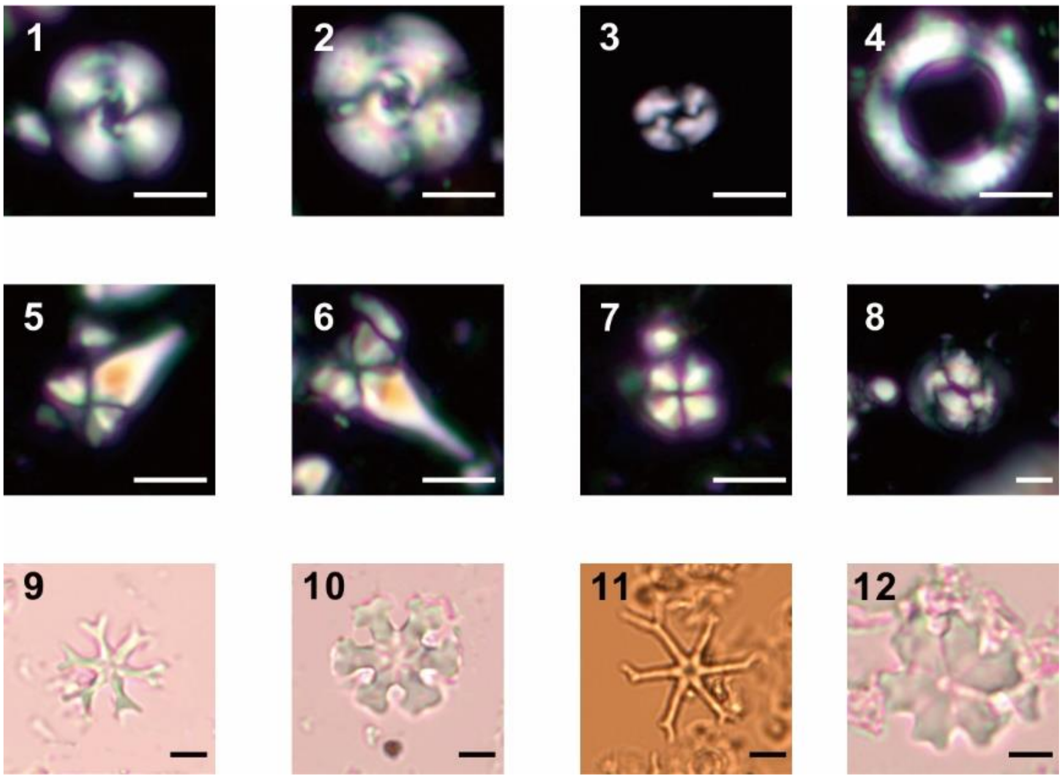

Figure S-2 Calcareous nannofossils in core FDZ050. 1-2. *Cyclicargolithus floridanus* (1: 8cm; 2: 21 cm). **3.** *Reticulofenestra* spp. (8 cm). **4.** *Coronocyclus nitescens* (21 m). **5-6.** *Sphenolithus heteromorphus* (first appearance (FA): 17.71 Ma, last appearance (LA): 13.53 Ma. 5: 8 cm; 6: 21 cm). **7**. *Sphenolithus moriformis* (21 cm). **8.**

Coccolithus pelagicus (21 cm). **9.** *Discoaster exilis* (21 cm). **10.** *Discoaster deflandrei* (21 cm). **11.** *Discoaster signus* (FA: 15.85 Ma, 8 cm). **12**. *Discoaster deflandrei* (8 cm). (Scale bar = 5 µm. 1-8: cross-polarised light; 9-12: transmitted light).

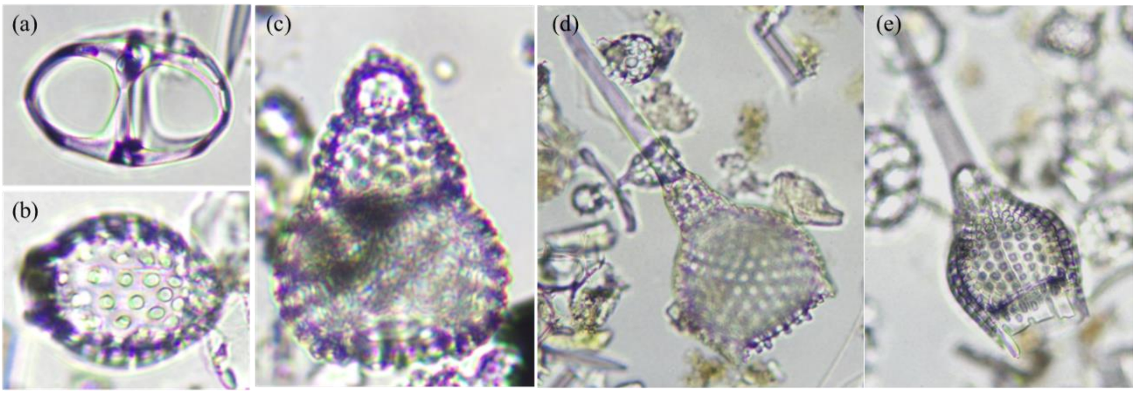

Figure S-3 Radiolarian fossils in core FDZ050 (12 cm depth) (a) *Trissocyclus stauroporus* (LA: 15.03 Ma). **(b)** *Carpocanium rubyae* (LA: 13.62 Ma). **(c)** *Eucyrrtidium diaphanes* (FA: 22.95 Ma, LA: 14.75 Ma). **(d)** *Calocycletta virginis* (*Riedel et Sanfilippo*) (FA: 21.12 Ma, LA: 12.72 Ma). **(e)** *Calicycletta costata* (*Riedel*) (FA:17.60, LA:13.44).

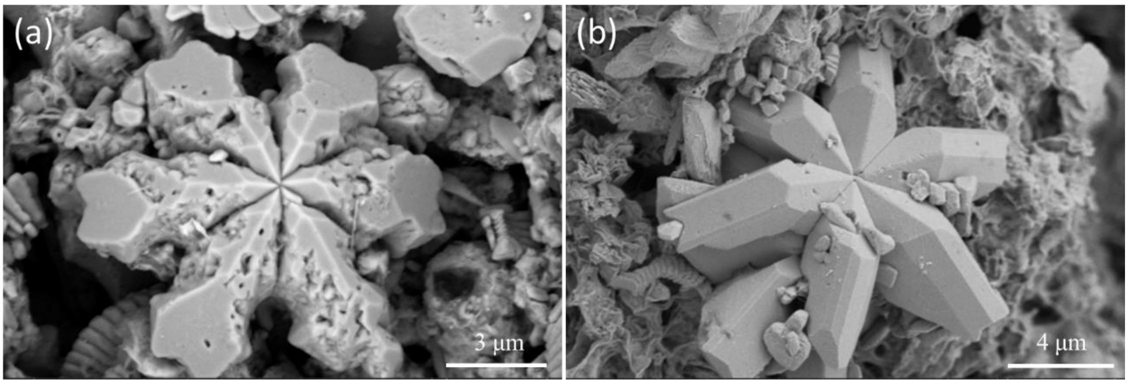

Figure S-4 *Discoaster spp.* from core FDZ050 exhibit varying degrees of dissolution. **(a)** Signifiant dissolution, 4 cm. **(b)** No dissolution, 21 cm.

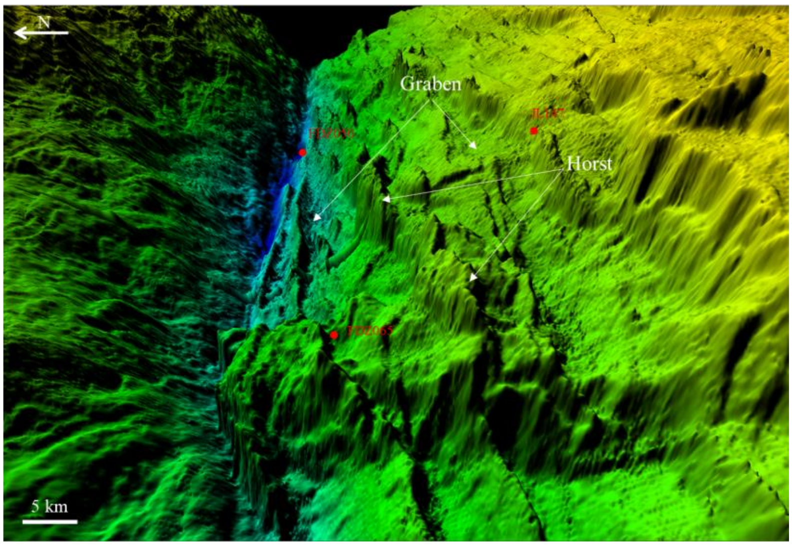

Figure S-5 3D topographic map in the Challenger deep area of the Mariana Trench.

Supplementary Information References

Bown, P.R. (1998) *Calcareous nannofossil biostratigraphy.* Springer, Netherlands.

Clift, P.D. (2017) A revised budget for Cenozoic sedimentary carbon subduction. *Reviews of Geophysics* 55, 97-125. https://doi.org/10.1002/2016RG000531

Gradstein, F.M., Ogg, J.G., Schmitz, M.D., Ogg, G.M. (2020) *Geologic time scale 2020*. First Edition, Elsevier, Amsterdam, Oxford, Cambridge.

Heiri, O., Lotter, A.F., Lemcke, G. (2001) Loss on ignition as a method for estimating organic and carbonate content in sediments: reproducibility and comparability of results. *Journal of Paleolimnology* 25, 101-110. https://doi.org/10.1023/A:1008119611481

McArthur, J.M., Howarth, R., Bailey, T. (2001) Strontium isotope stratigraphy: LOWESS version 3: best fit to the marine Sr-isotope curve for 0–509 Ma and accompanying look-up table for deriving numerical age. *The Journal of Geology* 109, 155-170. https://doi.org/10.1086/319243

Nigrini, C., Sanfilippo, A. (2001) Cenozoic radiolarian stratigraphy for low and middle latitudes with descriptions of biomarkers and stratigraphically useful species. *ODP Technical Note* 27.

Nigrini, C., Sanfilippo, A., Moore, T.J., Jr. (2005) Cenozoic radiolarian biostratigraphy: a magnetobiostratigraphic chronology of Cenozoic sequences from ODP Sites 1218, 1219, and 1220, equatorial Pacific. *Proceedings of theOcean Drilling Program Scientific. Results,* 199., 1–76. https://doi:10.2973/odp.proc.sr.199.225.2005

Plank, T., Langmuir, C.H. (1998) The chemical composition of subducting sediment and its consequences for the crust and mantle. *Chemical Geology* 145, 325-394. https://doi.org/10.1016/S0009-2541(97)00150-2

Qiu, Z., Zhang, L., Xiang, R., Zhang, Q., Hu, B., Chen, M. (2021) Biodiversity of radiolarians in surface sediments from the East Indian Ocean and their implication for water masses. *Deep Sea Research Part I: Oceanographic Research Papers* 177, 103625. https://doi.org/10.1016/j.dsr.2021.103625

Rea, D.K., Ruff, L.J. (1996) Composition and mass flux of sediment entering the world's subduction zones: Implications for global sediment budgets, great earthquakes, and volcanism. *Earth and Planetary Science Letters* 140, 1-12. https://doi.org/10.1016/0012-821X(96)00036-2

Robbins, L., Hansen, M., Kleypas, J., Meylan, S. (2010) CO2calc: A user-friendly seawater carbon calculator for Windows, Mac OS X, and iOS (iPhone). *US Department of the Interior, US Geological Survey*. https://doi.org/10.3133/ofr20101280